communications earth & environment

Article

A Nature Portfolio journal

https://doi.org/10.1038/s43247-026-03631-8

Mass flowering of the seagrass *Posidonia oceanica* after 2022 record-breaking marine heatwaves, a Pan-Mediterranean study

A list of authors and their affiliations appears at the end of the paper

Following the unprecedented marine heatwaves of summer 2022, extensive flowering of the endemic seagrass *Posidonia oceanica* was witnessed across the western Mediterranean. To unravel the causes of this event, we conducted a pan-Mediterranean analysis across 442 sites spanning all Mediterranean ecoregions, with 76% exhibiting flowering. Flowering differed regionally, with both highest flowering prevalence (over 90%) and flowering intensity (up to 0.75) recorded in the Liguro-Provençal and Balearic Seas. We demonstrate that regions experiencing large summer sea surface temperature anomaly with high marine heatwave cumulative intensity displayed the highest flowering intensity. The probability of flowering was very likely when marine heatwave cumulative intensity exceeded ~120°C days. These findings suggest that marine heatwaves trigger flowering in *P. oceanica* and, given the high energetic cost of sexual reproduction, continued ocean warming may shift energy allocation toward flowering. This shift could profoundly affect the species' reproductive strategies, posing major challenges and uncertainties for its long-term evolution.

Ongoing ocean warming and marine heatwaves (MHWs) are dramatically impacting coastal foundation species, including kelp forests, seagrasses, corals, and many invertebrates[1,2]. MHWs are becoming increasingly frequent and severe globally[3]. Summer 2022 saw record-high MHWs in the Mediterranean Sea[4,5], resulting in mass mortality events of many sessile benthic organisms[6,7]. The mean Sea Surface Temperature (SST) anomaly ranged between 1.3 and 2.6 °C above the long-term average (1982–2011)[4], reaching up to 4.6 °C in some areas of the western Mediterranean, which are record-breaking thermal conditions obtained over the past four decades[8] (Supplementary Fig. 1).

Seagrasses' primary strategy for meadow maintenance, growth, and recovery to disturbance is through vegetative horizontal clonal growth[9,10] and sexual reproduction, with frequencies and intensities that can vary significantly within and among species, leading to infrequent but massive and synchronized reproductive efforts[11]. Flowering in *Posidonia oceanica*, a foundational species endemic to the Mediterranean, has been rarely documented over the past century[12]. Nevertheless, sexual reproduction is crucial for introducing new genetic material necessary for evolutionary processes. Still, flowering is energetically costly[13], with P. oceanica needing to store starch and nutrients in its rhizomes over two to three years before undergoing flowering[14]. Flowering is sometimes massive and synchronized, which may be stimulated by elevated Summer SST[15], and could also reflect a reproduction strategy of producing a large quantity of fruits to saturate predators[16]. A greater investment in sexual reproduction may shift energy from other vital processes such as shoot growth, clonal propagation[13]; potentially disrupting the balance of the meadow and compromising its long-term ecosystem functioning and resilience. Since flowering patterns of marine and terrestrial plants are highly sensitive to environmental factors, particularly temperature[17,18], it is critical to understand how extreme thermal events impact these coastal foundation species, which play a paramount role in biodiversity, climate regulation, and the provision of essential ecosystem services, as is the case for *P. oceanica* in the Mediterranean Sea[19].

Here, we provide a pan-Mediterranean quantification of flowering records on *P. oceanica* following the record-breaking summer of 2022 across 442 sites (Supplementary Fig. 2). We assessed the spatial distribution of flowering, characterized summer thermal conditions using high-resolution satellite-derived SST data, and examined potential links with both biotic (e.g., meadow structure) and abiotic (e.g., depth, management level, temperature) factors. Additionally, we compared flowering intensity (proportion of shoots bearing an inflorescence) between the 2022 event and the Mass Flowering Event (MFE) that followed the intense 2003 MHW in the western Mediterranean[12]. Understanding shifts in reproductive strategies

e-mail: patrick.astruch@univ-amu.fr

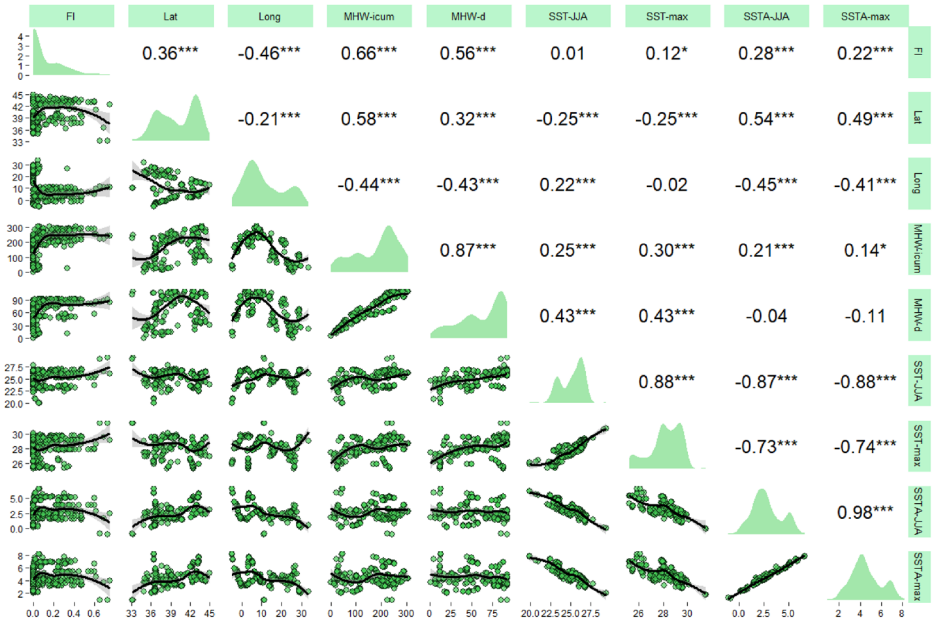

Fig. 1 | Spearman correlation matrix of flowering intensity, geographic coordinates, and thermal variables. Correlation matrix (Spearman test) between Flowering Intensity (FI, proportion of shoots with inflorescences), latitude (Lat, decimal degree), longitude (Long, decimal degree), Marine heatwave cumulative intensity (MHW-icum, °C day), MHW duration (MHW-d, day), Sea Surface Temperature in June July and August (SST-JJA, °C), maximum SST (SST-max, °C), SST Anomaly (SSTA-JJA, °C), SSTA-max (°C). Lower panels show scatterplots with Loess smoothing (in black) and 95% confidence intervals (light gray), upper panels show Spearman correlation coefficients, and diagonal panels display variable distributions. *$p < 0.05$; **$p < 0.01$; ***$p < 0.001$.

Table 1 | Synthesis of the quantitative data records per Mediterranean ecoregion

Ecoregions	*n*	mean FI	SD FI	Min FI	Max FI	FP
1-Alboran Sea	30	0.08	0.11	0	0.37	63%
2.1-Balearic Sea	133	0.21	0.14	0	0.48	93%
2.2-Liguro-Provençal (NW Med)	156	0.19	0.15	0.01	0.75	100%
2.3-Tyrrhenian Sea	20	0.14	0.19	0	0.61	63%
3-Adriatic Sea	25	0	0	0	0	0%
4-Ionian Sea	14	0.01	0.02	0	0.04	25%
5-Tunisian Plateau	4	0.60	0.19	0.32	0.73	-
6-Aegean Sea	59	0.02	0.05	0	0.33	30%
7-Levantine Sea	1	0.05	-	0.05	0.05	-
Total	442	0.15	0.16	0	0.75	76%

FI flowering intensity, *FP* flowering prevalence, *SD* standard deviation.

offers key insights into plant resilience and evolution in the face of climate change, at a time when accelerated change in the Mediterranean basin is particularly critical.

Results

Flowering data were obtained from all nine Mediterranean ecoregions (Supplementary Data 1): 159 records from the Liguro-Provençal ecoregion, 134 records from the Balearic Sea, 60 records from the Aegean Sea and 30 from the Alboran Sea. The other ecoregions were represented by fewer records: 27 from the Tyrrhenian Sea, 26 from the Adriatic Sea, 16 from the Ionian Sea, 7 from the Levantine Sea and 4 from the Tunisian Plateau (Supplementary Table 1).

Thermal regimes and warming trends in the Mediterranean

The Mediterranean Sea exhibits strong seasonality with an annual SST amplitude > 10 °C, also undergoing wide east-west and north-south gradients, as summarized by the climatological data for the different ecoregions (Supplementary Fig. 1A). The year 2022 was the warmest for the Mediterranean since the beginning of satellite SST records in 1982 (mean = 20.81 °C), 0.91 °C above the 1982–2021 average (Supplementary Fig. 1B). The highest anomalies were detected in the western Mediterranean, particularly during the meteorological summer (June, July and August, hereafter JJA) with mean SST Anomalies (SSTA) 2.42 °C above the 40-year average (Supplementary Fig. 1B).

Significant correlations were detected between MHW, SST, and SSTA descriptors (Spearman test: $p < 0.001$; Fig. 1). MHW cumulative intensity (MHW-icum) was positively related to summer SST in June-July-August (JJA) and positively related to SSTA-JJA (Spearman test: $p < 0.001$; Fig. 1), while SSTA-JJA was negatively related to SST-JJA (Spearman test: $R = -0.856$; $p < 0.001$), highlighting that the highest anomalies occurred in colder regions (e.g., Liguro-Provençal).

Flowering prevalence and intensity

Following the summer of 2022, flowering occurred in 333 out of the 442 sites monitored, corresponding to a Flowering Prevalence (FP: number of records reporting flowering in relation to the total number of records) of 76%. The highest FP values were observed in the Liguro-Provençal region and the Balearic Sea. Intermediate FPs were observed in the Alboran and Tyrrhenian Seas. The Aegean and Ionian Seas were characterised by low FPs, while no flowering was recorded within the Adriatic Sea (Table 1, Fig. 2).

The overall mean Flowering Intensity (FI; proportion of shoots bearing inflorescence in relation to the total nuÁmber of shoots) was 0.15 ± 0.16 across the whole Mediterranean basin, ranging between 0 (e.g., Adriatic Sea) and 0.75 (Giglio Island, Tuscany, Liguro-Provençal ecoregion). Strong differences in FI were observed between ecoregions ($p < 0.001$; Fig. 2, Supplementary Table 2), particularly between western and eastern ecoregions (pairwise test, $p < 0.05$). A higher mean FI was observed in the Tunisian Plateau with 0.60 ± 0.19 ($n = 4$ records), followed by the Balearic Sea, the Liguro-Provençal ecoregion, and the Tyrrhenian Sea. The mean FI was low in the Alboran Sea and very low in the Aegean and Ionian Seas (Figs. 2, 3; Table 1).

There was no significant influence of meadow structure category ($p = 0.062$), depth ($p = 0.056$), nor Management level ($p = 0.111$) on FI across ecoregions (i.e., Alboran Sea, Balearic Sea, Liguro-Provençal and Tyrrhenian Sea). Shoot density and FI did not exhibit any significant correlation across western ecoregions (Alboran Sea, Balearic Sea, Liguro-Provençal and Tyrrhenian Sea; Spearman test: $R = -0.03$, $p = 0.649$).

Relationships between marine heatwave descriptors and the mass flowering event

MHW-icum and marine heatwave duration (MHW-dur) were significantly correlated with FI ($R = 0.523$ and $R = 0.449$, respectively; $p < 0.001$) (Fig. 1).

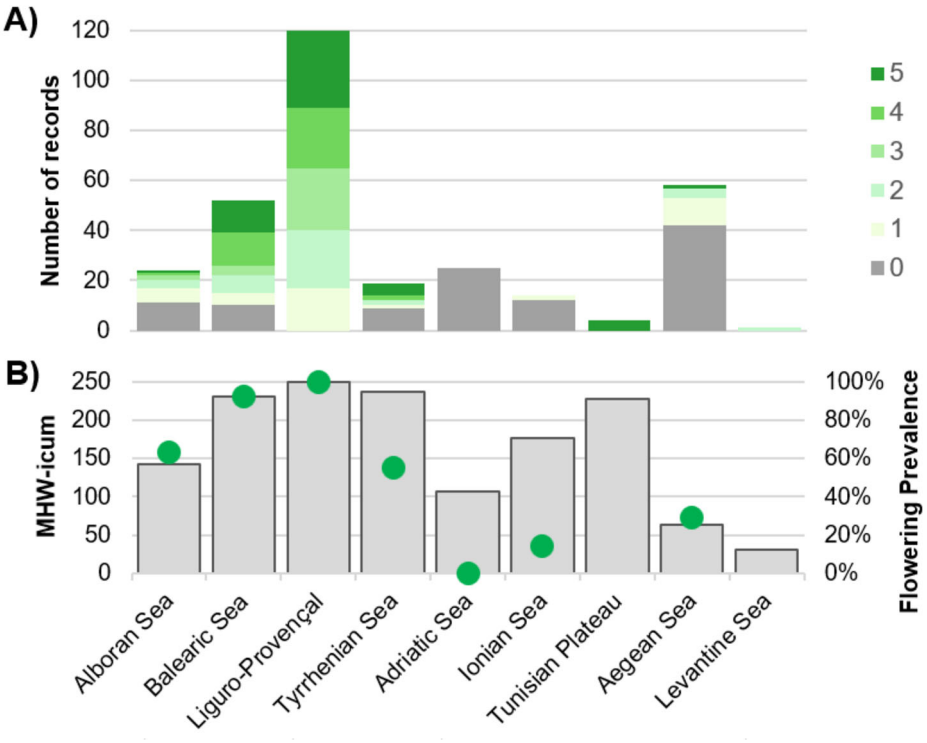

Fig. 2 | Flowering intensity records and marine heatwave cumulative intensity across Mediterranean ecoregions. A Number of records per Flowering Intensity (FI) level (0: No flowering; 1: Isolated flowering; 2: Small flowering; 3: Moderate flowering; 4: Large flowering; 5: Exceptional flowering; see Supplementary Table 3 for definitions), and (**B**) Marine heatwave cumulative intensity (MHW-icum, in °C days, grey columns) and Flowering Prevalence (%; FP, green dots, no data for Tunisian Plateau and Levantine Sea) per ecoregion.

The extent of the 2022 MFE exhibited strong spatial overlap with the exceptional MHWs, which occurred at subregional scales during summer, covering most of the western Mediterranean, the Alboran Sea, and the Tunisian Plateau (Fig. 2, Fig. 3). Analysis of local thermal conditions for the flowering records ($n = 442$) indicates that flowering ($n = 333$) occurred preferentially under the warmest conditions (Fig. 4), with a probability of flowering higher than 50% when MHW-icum exceeds 120 °C days (Supplementary Fig. 3).

The analysis of FI quantitative data above zero ($n = 193$) highlighted contrasted patterns depending on thermal conditions. Most of the records exhibiting moderate to large FI level (3, 4 or 5 FI level; $n = 126$, mean = 0.29 ± 0.16) were associated with elevated MHW-icum (mean = 246 ± 72 °C days). In contrast, large scatter of thermal exposure (mean = 180 ± 72 °C days) was found for small and isolated flowering (1 or 2 FI levels; $n = 82$, mean = 0.05 ± 0.16). When flowering was absent (FI = 0; n = 110), thermal exposure was found lower (mean = 128 ± 75 °C days).

To explore spatial variation in *P. oceanica* FI across the Mediterranean, we modelled continuous FI values as a function of mean summer SST (SST-JJA) and cumulative marine heatwave intensity (MHW-icum), while accounting for inherent baseline temperature differences among the different Mediterranean ecoregions (Fig. 5A). Our results reveal a positive relationship between thermal anomalies and flowering: both SST-JJA and MHW-icum were positively associated with FI across the dataset, with variations across regions. The highest MHW-icum values were recorded over the Tyrrhenian Sea, corresponding to some of the most intense flowering events observed. Similarly, the Balearic Sea and the Tunisian Plateau experienced both high MHW-icum and SST-JJA values, which also coincided with substantial flowering. These findings suggest that the most extreme flowering events may arise from the combined influence of high SST-JJA and elevated MHW-icum. Region-specific modelling further showed that all intercepts were negative (Fig. 5B), indicating that baseline flowering was generally unlikely in the absence of strong thermal forcing, particularly in western regions. In contrast, the slope estimates for both SST-JJA and MHW-icum were predominantly positive (Fig. 5C, 5D), reinforcing the role of thermal anomalies in driving flowering. The regional slopes in Fig. 5B–D reflect variation in the strength of the flowering response to MHW-icum across ecoregions. For SST-JJA and the intercept, 75% credible intervals did not cross zero, making these coefficients interpretable. Credible intervals for MHW-icum were wider and often including zero, reflecting greater uncertainty and contrasting trends among regions. Positive regional slope values indicate that flowering in that region responds more strongly to thermal anomalies than the entire Mediterranean.

Comparison with the 2003 Mass Flowering Event (western Mediterranean) and other historical records

To further contextualize our findings, we compared our results with the historical MFE of *P. oceanica* reported for the western Mediterranean in 2003[12] completed by additional historical records available from 1982-2001[12] and 2009-2021[20]. Analysis of SSTA-JJA in the western Mediterranean from 1982 to 2022 (Fig. 6A) revealed that both 2003 and 2022 were characterized by anomalously high summer SST, exceeding the historical range of the 1982–2021 time series. Summers 2022 and 2003 ranked as the warmest and 2nd warmest, respectively, since 1982 (26.10 °C and 25.84 °C, respectively). Median SSTA-JJA values during these two years reached 2.53 °C [Q25: 1.96 °C, Q75: 2.80 °C] and 2.12 °C [Q25: 1.72 °C, Q75: 2.55 °C] for 2022 and 2003 respectively (Fig. 6A). Consistent with our earlier analysis, high-intensity flowering in 2003 was associated with MHW-icum values above 150 °C days [182 ± 9 °C days] (Fig. 6B), closely aligning with the probability identified in our 2022 dataset (Fig. 6C). However, it is worth noting that the sparse historical records from 1982-2021 (excluding 2003) are associated with low MHW-icum (Fig. 6B; mean = 26 ± 40 °C days), confirming the exceptional nature of 2003 and 2022 MFEs and MHWs (Fig. 6A).

Discussion

Our study highlights an exceptional basin-wide flowering of *P. oceanica* in the aftermath of the 2022 MHWs, eclipsing the benchmark 2003 heatwave[21] and its associated MFE in the north-western Mediterranean[22]. Based on the currently available historical records[12,20], the 2022 event appears to be one of the most intense flowering events ever documented for this species. Despite strong differences among ecoregions, flowering after summer 2022 was observed in 76% of the study sites, with 90 to 100% occurrences for western

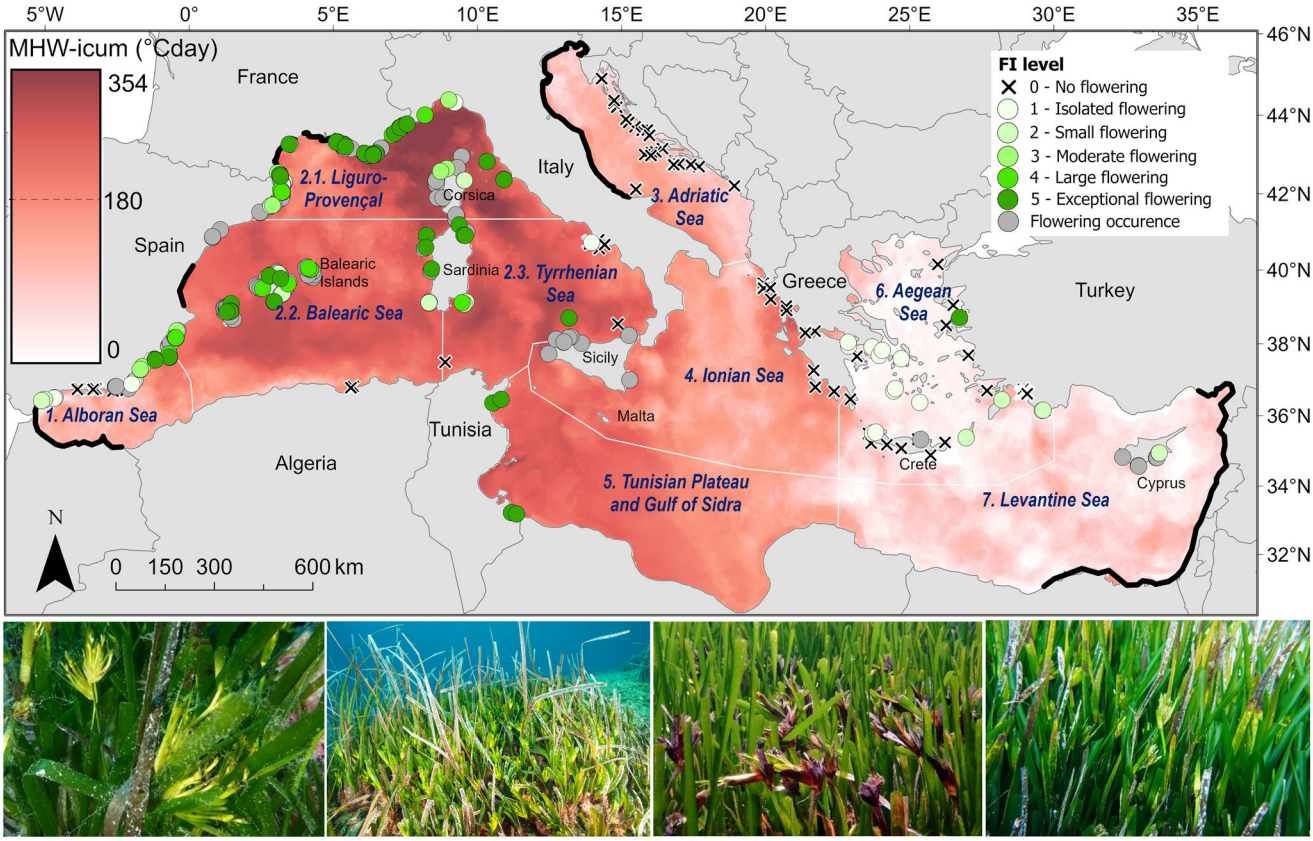

Fig. 3 | Location of 2022 flowering records within the Mediterranean basin. Flowering Intensity (FI, proportion of shoots bearing an inflorescence per total number of shoots. FI levels: 0: No flowering; 1: Isolated flowering; 2: Small flowering; 3: Moderate flowering; 4: Large flowering; 5 Exceptional flowering (see Supplementary Data 1 for more details). Flowering occurrence (in grey) corresponds to presence data of flowering. The black lines indicate areas without *P. oceanica* living meadows (Telesca et al.[57], Tutar et al.[42]). MHW-icum (°C day) is displayed across the Mediterranean basin for the period between 1st June and 31st August 2022. Photographs (from left to right): Provence, France (©Bruno Belloni); Corsica, France (©Tristan Estaque); Balearic Islands, Spain (©Jonathan Delgado); Ionian Sea, Greece (©Daniele Ventura). Leaves are approximately 0.8 to 1 cm wide.

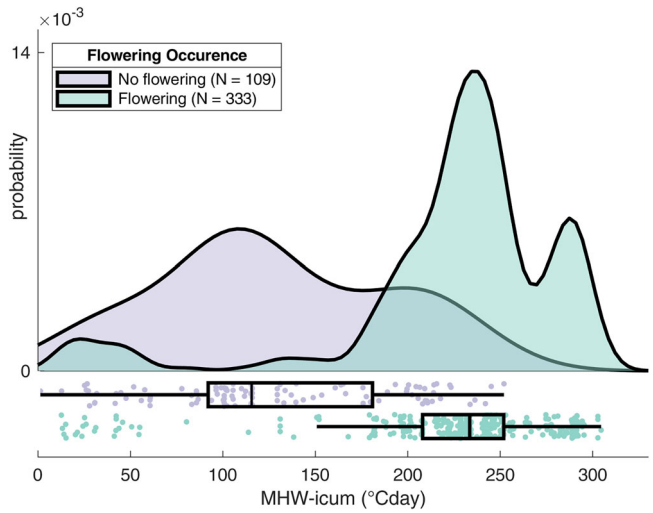

Fig. 4 | Probability of floweringg occurrence accordig to marine heatwave cumulative intensity. Relative distribution of the marine heatwave cumulative intensities (MHW-icum; °C day) associated with the probability of *Posidonia oceanica* flowering occurrence (i.e., observation of a flowering event).

Mediterranean regions. Flowering intensity (FI) reached 0.15 across the Mediterranean, with the highest values in the Tunisian Plateau and the western basin (up to 0.73 and 0.75 respectively), far higher than previous maximum FIs recorded in 2003 (i.e., 0.54 in the Balearic Islands; see ref. 12). Eastern regions such as the Aegean and Ionian Seas underwent lower FI (up to 0.01 to 0.04 respectively). We also showcase that the probability of flowering was very likely when MHW-icum exceeded ~120 °C days, raising questions about *P. oceanica*'s reproductive strategies and patterns in the face of global change.

While *P. oceanica* can flower yearly, flowering is usually sparse and localized[23], but large-scale flowering events have been observed throughout the past decades across the Mediterranean. However, the event observed in 2022 is unprecedented in terms of both intensity and scale. For instance, meadows that flowered intensively between 1957 and 2004 exhibited an average FI of 0.11 ± 0.02, with a maximum of 0.54[12]. In our study, FIs surpassed this value in numerous locations, exceeding 0.60 in Tunisia, Sardinia, Tuscany and Provence, highlighting the magnitude of the 2022 MFE. Furthermore, unprecedented FI values (up to 0.06) were recorded in 2022 in the westernmost part of *P. oceanica*'s distribution range (i.e., Southern Spain).

In the context of warming oceans, temperature appears to be a key driver of *P. oceanica* flowering[12,18,24–27]. Although the exact physiological mechanisms and triggers remain unresolved, the strong link between MHW-icum and flowering intensity supports the hypothesis that prolonged elevated temperature are necessary to trigger *P. oceanica* MFE. When the MHW-icum exceeded 150 °C days or more, FI was high (i.e., > 0.1) and regionally widespread (> 60% of records). In contrast, low FI values, such as those observed in previous works (e.g., see refs. 12,20), coincided with low MHW-icum (e.g., up to 75 °C days for 2010 in the Greek Seas[20]). The importance of temperature for flowering is well-documented in terrestrial plants, which is also influenced by photoperiod, light quality, and other factors[28]. Besides

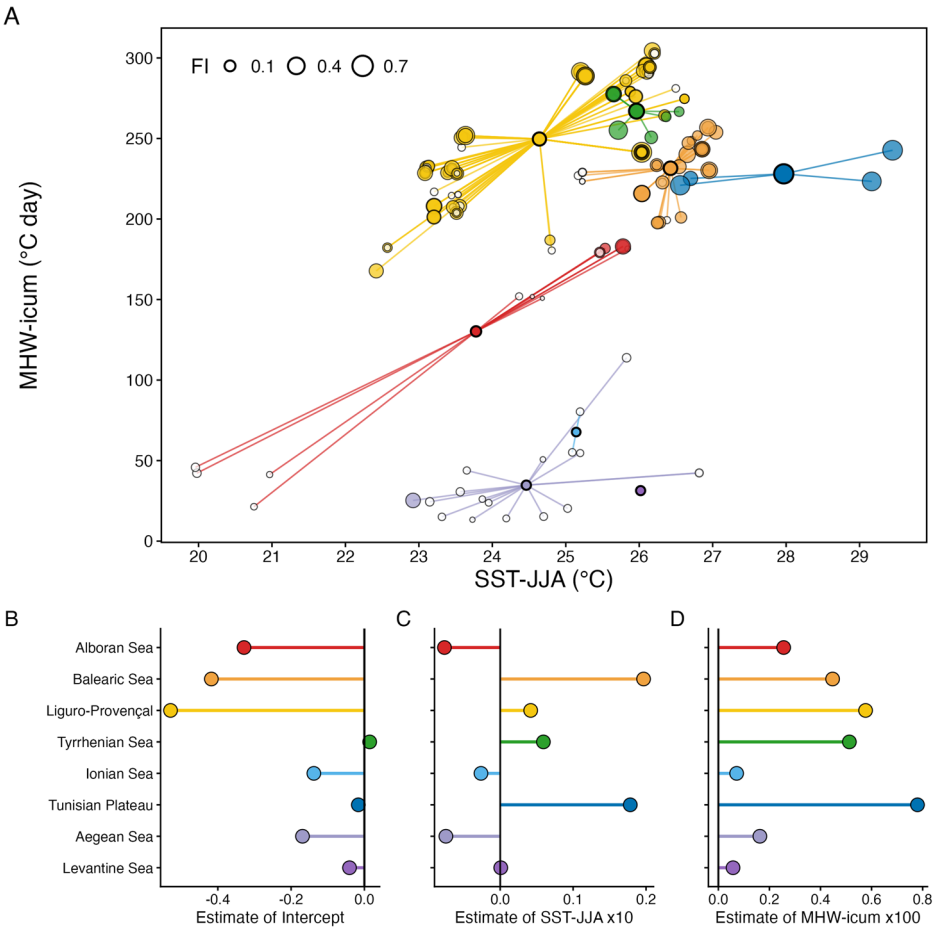

Fig. 5 | Relationships between flowering intensity (FI), summer sea surface temperature (SST-JJA), and cumulative marine heatwave cumulative intensity (MHW-icum) across nine Mediterranean ecoregions. A Three-dimensional scatterplot illustrating the relationships among FI, SST-JJA, and MHW-icum. Each point represents a site, scaled by FI magnitude and connected to its corresponding regional centroid. No FI observations are filled in white. **B**–**D** Standardized random-effect deviations from the hierarchical Bayesian model of logit-transformed FI as a function of SST-JJA and MHW-icum (see Online Methods section 4.3, Eq. 8). These values represent how much each ecoregion departs from the global intercept or global slopes, expressed in standard deviation units: (**B**) deviation from the global intercept, (**C**) deviation from the global SST-JJA effect, (**D**) deviation from the global MHW-icum effect. Colours denote regions: Alboran Sea (red), Balearic Sea (orange), Liguro-Provençal Basin (yellow), Tyrrhenian Sea (green), Adriatic Sea (light green), Ionian Sea (light blue), Tunisian Plateau (dark blue), Aegean Sea (light purple), and Levantine Sea (dark purple).

ocean warming, SST increases are also linked to solar activity cycles[29], which also impact various biological processes. Indeed, peaks in *P. oceanica* flowering every 9–11 years correlate with solar cycles[12,30] and, in fact, the 2022 flowering event, occurring 10 years after the sunspot peak of 2012, was predicted based on this pattern[30] (Supplementary Fig. 4). However, recent solar cycles (e.g., of 2022–2024) were weaker (150–160 sunspots per month) than the solar cycles peaking in 2000–2002 (> 200 sunspots per month; Supplementary Fig. 4), after which the 2003 MFE occurred[12]. Such a decrease in solar intensity, combined with increasing flowering events, suggests that rising temperatures driven by climate change are likely playing a key role in influencing mass flowering. Elevated temperatures can affect plant metabolism and, consequently, influence the ability of *P. oceanica* to accumulate reserves[31,32]. In fact, observations of mass beach-cast *P. oceanica* fruits and seeds have been reported for the Warm Roman Period (i.e., from ca 250 BCE to 400 CE[33]) in southeast Spain, and central and southern Italy. Unfortunately, quantitative information is lacking for the Little Ice Age (ca. 1300–1850 CE) which underwent particularly cold thermal conditions[34] and only some flowering records are available for that age (e.g., Provence, Tyrrhenian Sea, Adriatic Sea, Sardinia, Algeria, southeast Spain; see refs. 12), which in turn might underline the strong relationship between high thermal conditions and MFE.

Flowering is metabolically costly, and *P. oceanica* plants accumulate reserves (starch) about two years prior to flowering[13,30]. These temporal dynamics may help explain the low flowering observed in 2022 in the Tyrrhenian Sea and the Aegean Sea, where high fruit and seed beaching (in the Tyrrhenian Sea[35]) and widespread flowering (in Greek waters[20]) occurred in 2021. However, it is worth noting that mass flowering still follows an endogenous rhythm of the plant, which is not directly induced but regulated by environmental factors including solar activity[36]. Continuous warming, as seen in other biological systems, could disrupt synchrony and endogenous rhythm[37]. Given that temperature drives reserve accumulation and flowering events are becoming more intense (see refs. 12,27; present work), *P. oceanica* flowering patterns may no longer strictly follow solar cycles.

Interestingly, no flowering was observed after summer of 2022 in the Adriatic Sea, the last flowering being observed in 2011[38], although recent very localised flowering and fruit production was observed in early winter 2024 in Biševo Island (Croatia, Jelena Kurtović pers. obs.). However, following summer 2024 MHW, an unprecedented MFE has occurred along the Italian coast of the Adriatic Sea and in Montenegro (see ref. 27; Vesna Mačić pers. obs.). The drivers of such flowering patterns remain to be understood, but genetic composition and structure of seagrass populations are also likely influencing flowering patterns at different spatial scales. High genetic relatedness and heterozygosity have been linked to greater inflorescence abundance in *P. oceanica*[39]. Two main genetic groups exist in the western and eastern basins, probably resulting from past glaciation events that limited gene flow[40]. These groups exhibited distinct flowering patterns in 2022, with genetic differences within regions such as the Tyrrhenian Sea[41], the Aegean and the Levantine Seas[42,43] and the Adriatic Sea[44]. Additionally, *P. oceanica* cuttings and seedlings obtained from 13 different localities across the Mediterranean were planted at Port-Cros National Park (Provence, France) in the frame of a transplant experiment in 1987[45]. In 2022, all transplanted patches flowered, but FI varied significantly by origin with 0.01 for cuttings from Malta (Ionian Sea) and 0.79 for those from Mallorca (Balearic Sea) (Heike Molenaar pers. obs.), highlighting the key role of genetics in influencing flowering patterns.

MFEs do not always lead to significant fruiting the following spring[46,47]. After the 2022 MFE, beach-cast fruits and seeds were seen in southern France, but abortion (i.e., interrupted development of inflorescences and fruits) occurred at several sites[24,48]. Furthermore, successful recruitment of seedlings is very low[49,50] and young seedlings and plantlets have a lower

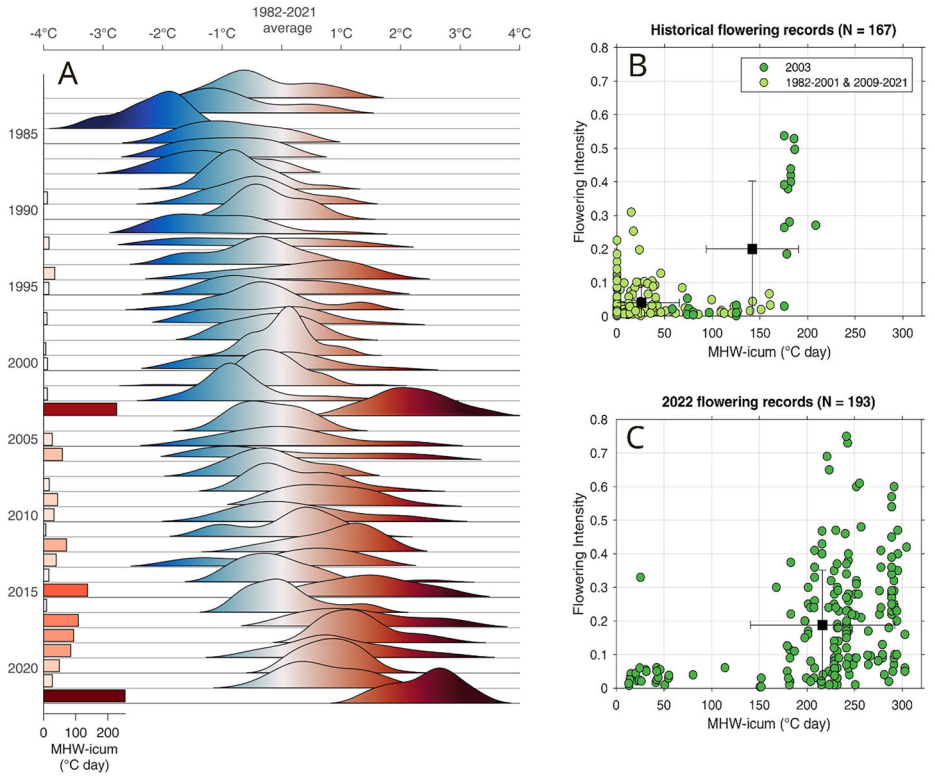

Fig. 6 | Summer thermal anomalies, marine heatwaves, and flowering intensity relationships. **A** Summer daily sea surface temperature anomaly (SSTA in °C, referenced to the period 1982–2021) and marine heatwave cumulative intensities (MHW-icum in °C day) from 1982 to 2022 in the western Mediterranean; Flowering Intensity (FI) in relation to MHW-icum for: (**B**) 2003 in dark green and 1982–2001 and 2009–2021 in light green (from Diaz-Almela et al. 2007 and Garcia-Escudero et al., 2024) and for (**C**) 2022 (present work). The mean ± standard deviation values are shown in black.

tolerance threshold to warming than adult plants[51,52]. Therefore, many seedlings may not survive frequent MHWs, potentially preventing the benefits of mass flowering.

The increased flowering observed in the last years could suggest that the species is now encountering better thermal conditions and that sexual reproduction will positively bolster population genetic variability and resilience. Nevertheless, the assumption that *P. oceanica* is benefiting from seawater warming remains a speculation. The complete picture should be considered, including the metabolic investment and carbon balances in the face of more frequent sexual events, and the possible drawback on the resilience of flowering clones. Indeed, MHWs can cause widespread mortality of *P. oceanica* meadows[53,54] and mass flowering after warming has been interpreted as a stress-triggered strategy to compensate for mortality by promoting recruitment, dispersal, and greater genetic diversity to support adaptation under warming conditions[55,56]. A better understanding of shifts in reproductive strategies is critical not only for uncovering plant resilience and adaptive potential but also for conservation efforts as the Mediterranean undergoes accelerated ecological transformation[57].

Online Methods

Assessment of the 2022 Mass Flowering Event across the Mediterranean

Spatial extension of the study. A comprehensive database covering the entire Mediterranean basin was established to document the flowering occurrences following summer 2022 marine heatwaves (MHWs). More than a hundred people from 10 countries and 47 teams (Non-Governmental Organisations, universities, research laboratories, marine protected areas (MPAs)) were involved. A total of 463 records were collected from the sea surface to 25 m depth, between latitudes ranging from 33.19°N to 44.91°N and longitudes ranging from 5.12°E to 33.66°E. A meadow structure category was assigned to each site when the information was available in order to test its influence on flowering patterns, specifically: (i) naturally fragmented (e.g., meadow cover under 80%, see ref. 58), (ii) fragmented by anthropogenic pressures (e.g., anchoring, other mechanical degradation, low water quality), and (iii) continuous (over 80% of meadow cover). Records were collected from areas under different levels of management: (i) areas without regulation, (ii) MPAs, most of them Natura 2000 sites (EU Habitat Directive, 92/43/CEE) without significant management measures; (iii) intermediate level of protection, involving conservation measures and regulation of most of the human activities (e.g., small-scale fishing, anchoring – Multi-Use-Management) and (iv) No-Entry Zones (i.e., fully protected areas). Compiled data included qualitative, semi-quantitative and quantitative estimates of flowering obtained between September 2022 and July 2023, spanning the entire sequence from inflorescence formation to fruit dispersal.

Sampling sites were classified according to the Marine Ecoregions of the World[59]: 1: Alboran Sea; 2: Western Mediterranean; 3: Adriatic Sea; 4: Ionian Sea; 5: Tunisian Plateau and Gulf of Sidra (hereafter 'Tunisian Plateau'); 6: Aegean Sea; 7: Levantine Sea. For the purpose of this work, and given the extensive sampling effort in the western Mediterranean (zone 2), this ecoregion was divided into three sub-regions: 2.1 Balearic Sea, 2.2 Liguro-Provençal and 2.3 Tyrrhenian Sea (adapted from ref. 60; Supplementary Fig. 5).

Types of flowering data

Qualitative records (n = 41). When flowering or fruiting was observed for a given site, at least the date and the geographical coordinates were recorded. Null occurrence records, corresponding to the absence of flowering in a site, were also noted.

Semi-quantitative records (n = 186). The magnitude of flowering was assessed using the following categories: (I) Isolated flowering, (II) Small flowering, (III) Moderate flowering, (IV) Large flowering, (V) Exceptional flowering (See Supplementary Table 3[61]). Available in situ photographs were also used to estimate flowering density categories, when available. The record was also considered as semi-quantitative if less than three replicates from quantitative records were available for a given site (n = 18 sites).

Quantitative records (n = 236). The number of living shoots and the number of inflorescences were counted within a quadrat randomly replicated at least three times in the meadow. The number and size of quadrats differed according to the data provider, but were always of standardized size (e.g., 20 cm x 20 cm, 25 cm x 25 cm, 25 cm x 30 cm, 40 cm x 40 cm), enabling a density estimation per m². Lepidochronological analysis data (i.e., rhizome analysis for annual growth rate and sheet production allowing the identification of floral stalks and an estimation of the flowering intensity (FI); see ref. 62) were also considered (Supplementary Fig. 6). Sampling was conducted at different depths, ranging from 0 to 25 m, and three depth categories were considered following[48]: shallow (< 7.5 m), intermediate (between 7.5 and 12.5 m), and deep (> 12.5 m).

During data collection, 21 sites were not considered in the analysis as they corresponded to observations of beach-stranded inflorescences or fruits ($n = 14$; e.g., Sicily, Liguria, Corsica) or were based on reports lacking specific field observations ($n = 7$; e.g., Sicily, Montenegro). (Supp. Mat. 1).

Flowering prevalence and flowering intensity descriptors. Flowering Prevalence (FP) was estimated as the number of records reporting flowering in relation to the total number of records obtained throughout the study[12]. FP was calculated for each ecoregion that contained at least 10 records, as well as for the whole Mediterranean basin. Flowering Intensity (FI; see refs. 21,22) was estimated as the proportion of shoots bearing inflorescence in relation to the total number of shoots within the quadrats. To relate flowering density to total shoot density, a classification based on FI (hereafter FI level) was used (Supplementary Table 3). As Giraud's classification[61] and FI level are strongly correlated (Spearman test: $R = 0.965$, p-value < 0.001), FI level, more representative of actual flowering at each site, was used to display the results.

Thermal conditions and MHWs metrics

Temperature data set. In order to obtain accurate information throughout an extensive geographical area, SST time series over the Mediterranean Sea at 0.05° resolution grid were obtained from the Copernicus Marine Environment Monitoring Service (CMEMS, https://doi.org/10.48670/moi-00173[63,64]). The data consists of daily (night-time), optimally interpolated (level 4), satellite-based estimates of the foundation SST from January 1st 1982 to the end of 2022, reprocessed with increased stability and consistency for climate applications. Importantly, this dataset exhibited high agreement with near-shore in situ time series around the Mediterranean Sea and was found relevant for trends and extreme events analysis in the coastal zone[65].

Temperature data analysis. Individual SST analyses were conducted per pixel at 0.05° grid resolution. Following Hobday et al.[66], a MHW is defined as a prolonged (at least five consecutive days) and discrete warming event, when the local temperature exceeds the seasonally varying threshold defined on the basis of 30 years of climatology data. MHW metrics were computed using the Zaho & Marin[67] package for Matlab, with climatological mean and 90th percentile calculated over the 1982–2011 period. Seasonal MHW statistics were calculated by considering all MHW days (number of days when SST exceeds the 90th percentile threshold) during meteorological summer (from 1st June to the end of August each year – hereafter JJA). These three months correspond to the warm period that precedes the sexual reproductive phase. Summer MHW total duration (MHW-dur, in days) and cumulative intensity (MHW-icum, in °C day) were defined as the total of all MHW days and the sum of all MHW daily intensities (i.e., anomaly relative to the climatological mean), respectively.

Additional SST descriptors were calculated to assess their correlation with the flowering dataset: (i) maximum SST (SST_{max}), (ii) mean SST (SST_{mean}) and (iii) mean SST Anomaly (SSTA) with respect to the 1982-2021 average. SST_{mean} and SSTA were calculated considering two different time windows (yearly and for the summer season).

Comparison with 2003 flowering event and other available historical records. The dataset from Díaz-Almela et al.[12] on flowering records reported after the 2003 MHWs, was completed with authors' records, and was imported in numerical format and graphically analysed. The validated dataset consists of quantitative FI data for 24 sites for which nearest satellite SST time series were extracted and considered for MHW analysis. The dataset validated with original authors consists of 24 records (sites) for 2003 (available in Supplementary Data 1). In addition, historical records from 1982 to 2001 (from ref. 12; $n = 101$) and from 2009 to 2021 (from ref. 27; $n = 42$) were also considered for MHW analysis (Supplementary Data 1).

Statistical analysis

First, to test the effects of biotic and abiotic factors (ecoregions, depth, management level and meadow structure) on FI, PERMANOVAs[68] were conducted with 9999 permutations, completed by a pairwise test. Spearman tests were conducted to test the correlation between FI and biotic and abiotic factors.

Then, to evaluate the probability of flowering occurrence in *P. oceanica* during the 2022 event, we first applied a Bayesian modelling framework using a binomial distribution (Eq. 1). The response variable was coded as binary (1 = flowering observed, 0 = no flowering), and the single predictor variable included was the MHW cumulative intensity (MHW-icum) (Eq.2):

$$\text{Flowering} \sim \text{Bernoulli}(\mu_{\text{Flowering}}) \tag{1}$$

$$\mu_{\text{Flowering}} = \text{logit}^{-1}(\beta_0 + \beta_1 \times \text{MHW} - \text{icum}) \tag{2}$$

$$\beta_0 \sim \text{Student} - \text{t}(3,\ 0,\ 10); \beta_1 \sim \text{Student} - \text{t}(3,\ 0,\ 2.5) \tag{3}$$

Here, β_0 is the intercept and β_1 is the coefficient for MHW-icum. Both parameters were assigned Student-t priors, specified by three values: degrees of freedom (3), location (mean, 0), and scale (spread; 10 for β_0, 2.5 for β_1). These weakly informative priors allow the data to primarily drive the inference while limiting extreme values. We chose a Bayesian approach to fully propagate uncertainty in parameter estimates and to accommodate the hierarchical structure of the data. The model was implemented using the brms package[69] with four Markov chains of 4000 iterations each (1000 warm-up steps). Convergence was assessed via R-hat values (< 1.01)[70] and trace plots. We set adapt_delta = 0.99 and max_treedepth = 15 to ensure efficient and reliable sampling.

We further applied a second Bayesian approach to track flowering intensity continuously. Because FI is bounded between 0 and 1, values were logit-transformed, and a normal likelihood was applied on the transformed scale (Eqs. 4–7).

$$\text{FI} \sim \text{Normal}(\mu_{\text{FI}}) \tag{4}$$

$$\mu_{\text{FI}} = \beta_0 + \beta_1 \times \text{MHW} - \text{icum} + \beta_2 \times \text{SST} - \text{JJA} + \zeta_{\text{Ecoregion}} \tag{5}$$

$$\zeta_{\text{Ecoregion}} = (\Omega Z)\delta_s \tag{6}$$

$$\text{diag}(Z) = \sigma_\zeta \tag{7}$$

$$\beta_0 \sim \text{Student-t}(3, 0, 10); \beta_1, \beta_2, \delta_s \sim \text{Student-t}(3, 0, 2.5); \sigma, \sigma_\zeta \sim \Gamma(0.01, 0.01); \Omega \sim \text{LKJ}(1). \tag{8}$$

The model includes MHW-icum, SST-JJA and a vector of $n = 9$ levels of ecoregions observed. These vectors construct a hierarchical matrix ζ with n rows and two columns, representing ecoregion-level additive deviationns from β_0. In this model, Ω is the Cholesky factor of the correlation matrix among hierarchical effects, Z is a diagonal matrix with a vector of among-ecoregion standard deviations (σ_ζ), and δ_s is an s-by-two matrix of

standardized hierarchical effects. We ran the model with four chains, each with 4 000 draws and a warm-up period of 1000 steps, retaining 12 000 posterior draws for analysis. Models (1), and (4) displayed R^2 of 0.32 and 0.68 respectively. All statistical analyses were conducted using R v. 4.4.3[71].

Reporting Summary

Further information on research design is available in the Nature Portfolio Reporting Summary linked to this article.

Data availability

The full dataset is available in figshare (https://doi.org/10.6084/m9.figshare.32140954) and as an excel file: supplementary_data_1_dataset_2022-2021-1982_flowering_Posidonia_final.xlsx

Received: 1 September 2025; Accepted: 6 May 2026;
Published online: 22 May 2026

References

1. Garrabou, J. et al. Marine heatwaves drive recurrent mass mortalities in the Mediterranean Sea. *Glob. Change Biol.* **28**, 5708–5725 (2022).
2. Smith, K. E. et al. Global impacts of marine heatwaves on coastal foundation species. *Nat. Commun.* **15**, 5052 (2024).
3. Oliver, E. C. J. et al. Marine heatwaves. *Annu. Rev. Mar. Sci.* **13**, 313–342 (2021).
4. Guinaldo, T., Voldoire, A., Waldman, R., Saux Picart, S. & Roquet, H. Response of the sea surface temperature to heatwaves during the France 2022 meteorological summer. *Ocean Sci.* **19**, 629–647 (2023).
5. Marullo, S. et al. Record-breaking persistence of the 2022/23 marine heatwave in the Mediterranean Sea. *Environ. Res. Lett.* **18**, 114041 (2023).
6. Estaque, T. et al. Marine heatwaves on the rise: One of the strongest ever observed mass mortality event in temperate gorgonians. *Glob. Change Biol.* **29**, 6159–6162 (2023).
7. Grenier, M., Idan, T., Chevaldonné, P. & Perez, T. Mediterranean marine keystone species on the brink of extinction. *Glob. Change Biol.* **29**, 1681–1683 (2023).
8. Mercator Ocean International. Record-high marine heatwaves in the Mediterranean Sea, summer 2022. Mercator Ocean International. Retrieved the 15 September 2024 from https://www.mercator-ocean.eu/actualites/marine-heatwaves-mediterranean-summer-2022/ (2022).
9. Marbà, N. & Duarte, C. M. Rhizome elongation and seagrass clonal growth. *Mar. Ecol. Prog. Ser.* **174**, 269–280 (1998).
10. Di Carlo, G., Badalamenti, F., Jensen, A. C., Koch, E. W. & Riggio, S. Colonisation process of vegetative fragments of *Posidonia oceanica* (L.) Delile on rubble mounds. *Mar. Biol.* **147**, 1261–1270 (2005).
11. Cabaço, S. & Santos, R. Seagrass reproductive effort as an ecological indicator of disturbance. *Ecol. Indic.* **23**, 116–122 (2012).
12. Díaz-Almela, E., Marbà, N. & Duarte, C. M. Consequences of Mediterranean warming events in seagrass (*Posidonia oceanica*) flowering records. *Glob. Change Biol.* **13**, 224–235 (2007).
13. Gobert, S., Lejeune, P., Lepoint, G. & Bouquegneau, J. M. C, N, P concentrations and requirements of flowering *Posidonia oceanica* shoots. *Hydrobiologia* **533**, 253–259 (2005).
14. Calvo, S. et al. Modelling the relationship between sexual reproduction and rhizome growth in *Posidonia oceanica* (L.) Delile. *Mar. Ecol.* **27**, 361–371 (2006).
15. Bonal, R., Munoz, A. & Díaz, M. Satiation of predispersal seed predators: the importance of considering both plant and seed levels. *Evolut. Ecol.* **21**, 367–380 (2007).
16. Qin, L. Z. et al. Influence of regional water temperature variability on the flowering phenology and sexual reproduction of the seagrass *Zostera marina* in Korean coastal waters. *Estuaries Coasts* **43**, 449–462 (2020).
17. Ito, M. A., Lin, H. J., Connor, M. I. & Nakaoka, M. Large-scale comparison of biomass and reproductive phenology among native and non-native populations of the seagrass *Zostera japonica*. *Mar. Ecol. Prog. Ser.* **675**, 1–21 (2021).
18. Boudouresque, C. F. et al. The heatwave of summer 2022 in the north-western Mediterranean Sea: some species were winners. *Water* **16**, 1–19 (2024).
19. Vassallo, P. et al. The value of the seagrass *Posidonia oceanica*: A natural capital assessment. *Mar. Pollut. Bull.* **75**, 157–167 (2013).
20. García-Escudero, C. A. et al. Strong marine heatwaves trigger flowering in seagrass. *Limnol. Oceanogr.* **9999**, 1–14 (2024).
21. Garrabou, J. et al. Mass mortality in Northwestern Mediterranean rocky benthic communities: effects of the 2003 heat wave. *Glob. Change Biol.* **15**, 1090–1103 (2009).
22. Díaz-Almela, E. et al. Patterns of seagrass (*Posidonia oceanica*) flowering in the Western Mediterranean. *Mar. Biol.* **148**, 723–742 (2006).
23. Balestri, E. & Vallerini, F. Interannual variability in flowering of *Posidonia oceanica* in the North-Western Mediterranean Sea, and relationships among shoot age and flowering. *Botanica Mar.* **46**, 525–530 (2003).
24. Ruíz, J. M. et al. Experimental evidence of warming-induced flowering in the Mediterranean seagrass *Posidonia oceanica*. *Mar. Pollut. Bull.* **134**, 49–54 (2018).
25. Stipcich, P., La Manna, G. & Ceccherelli, G. Warming-induced flowering and fruiting in the seagrass *Posidonia oceanica* and uncertainties due to context-dependent features. *Mar. Biol.* **171**, 67 (2024).
26. Tomas, F. et al. Mass flowering and unprecedented extended pseudovivipary in seagrass (*Posidonia oceanica*) after a Marine Heat Wave. *Mar. Pollut. Bull.* **202**, 1–7 (2024).
27. Chimienti, G., Tursi, A., Maiorca, M. & Mastrototaro, F. Flowering of *Posidonia oceanica* in the Italian Adriatic Sea following the 2024 marine heatwave. *Estuar., Coast. Shelf Sci.* **324**, 109483 (2025).
28. Schauber, E. M. et al. Masting by eighteen New Zealand plant species: the role of temperature as a synchronizing cue. *Ecology* **83**, 1214–1225 (2002).
29. Roy, I. & Haigh, J. D. Solar cycle signals in sea level pressure and sea surface temperature. *Atmos. Chem. Phys. Discuss.* **9**, 25839–25852 (2009).
30. Montefalcone, M., Giovannetti, E., Morri, C., Peirano, A. & Bianchi, C. N. Flowering of the seagrass *Posidonia oceanica* in NW Mediterranean: is there a link with solar activity? *Mediterranean Marine Sci.* 416-423 (2013). https://doi.org/10.12681/mms.529
31. Marín-Guirao, L. et al. Carbon economy of Mediterranean seagrasses in response to thermal stress. *Mar. Pollut. Bull.* **135**, 617–629 (2018).
32. Litsi-Mizan, V. et al. Decline of seagrass (*Posidonia oceanica*) production over two decades in the face of warming of the Eastern Mediterranean Sea. *N. Phytologist* **239**, 2126–2137 (2023).
33. Lelli, E. Il tonno “Maiale del mare” da Polibio ad Ateneo. In: *Quaderni Urbinati di Cultura Classica New Series*, *Fabrizio Serra Editore* 78, 153-158 (2004).
34. Sicre, M. A. et al. Sea surface temperature variability in the North Western Mediterranean Sea (Gulf of Lion) during the Common Era. *Earth Planet. Sci. Lett.* **456**, 124–133 (2016).
35. Procaccini, G., Dattolo, E. & Ruocco, M. Genetic diversity and connectivity in the Mediterranean seagrass *Posidonia oceanica*: state of art and future directions. *Cah. de. Biologie Mar.* **64**, 105–114 (2023).
36. McWatters, H. G. & Devlin, P. F. Timing in plants–a rhythmic arrangement. *FEBS Lett.* **585**, 1474–1484 (2011).
37. Piao, S. et al. Plant phenology and global climate change: Current progresses and challenges. *Glob. Change Biol.* **25**, 1922–1940 (2019).
38. Mačić, V. Intensive fructification of *Posidonia oceanica* (L.) Del. on the coast of Montenegro (south-east Adriatic Sea). *Rapp. de. la Comm.*

Int. pour l'Exploration Scientifique de. la Mer. Méditerranée **40**, 521 (2013).
39. Jahnke, M. et al. Should we sync? Seascape-level genetic and ecological factors determine seagrass flowering patterns. *J. Ecol.* **103**, 1464–1474 (2015).
40. Serra, I. A. et al. Genetic structure in the Mediterranean seagrass *Posidonia oceanica*: disentangling past vicariance events from contemporary patterns of gene flow. *Mol. Ecol.* **19**, 557–568 (2010).
41. Procaccini, G., Orsini, L., Ruggiero, M. V. & Scardi, M. Spatial patterns of genetic diversity in *Posidonia oceanica*, an endemic Mediterranean seagrass. *Mol. Ecol.* **10**, 1413–1421 (2001).
42. Tutar, O. et al. High levels of genetic diversity and population structure in the Mediterranean seagrass *Posidonia oceanica* at its easternmost distribution limit. *ICES J. Mar. Sci.* **79**, 2286–2297 (2022).
43. Litsi-Mizan, V. et al. Unravelling the genetic pattern of seagrass (*Posidonia oceanica*) meadows in the Eastern Mediterranean Sea. *Biodivers. Conserv.* **33**, 257–280 (2024).
44. De Paola, D. et al. *Posidonia oceanica* meadows of the Italian southern Adriatic Sea display different genetic structure. *J. Nat. Conserv.* **78**, 126585 (2024).
45. Meinesz, A., Caye, G., Loques, F. & Molenaar, H. Polymorphism and development of *Posidonia oceanica* transplanted from different parts of the Mediterranean into the National Park of Port-Cros. *Botanica Mar.* **36**, 209–216 (1993).
46. Pergent, G. & Pergent-Martini, C. Phénologie de *Posidonia oceanica* (Linnaeus) Delile dans le bassin méditerranéen. Annales de. l'Inst. océanographique (Monaco) **64**, 79–100 (1988).
47. Sánchez-Lizaso, J. L. Inventario de las observaciones de floraciones y fructificaciones de *Posidonia oceanica* en el Mediterráneo ibérico. In: *Historia Natural'91*, Alemany, A. (edit.), 291-296 (1992).
48. André, S. et al. The 2022 mass flowering of *Posidonia oceanica* in the French Mediterranean Sea: is it unprecedented? *Sci. Rep. Port.-Cros Natl. Park* **37**, 65–100 (2023).
49. Balestri, E., Piazzi, L. & Cinelli, F. Survival and growth of transplanted and natural seedlings of *Posidonia oceanica* (L.) Delile in a damaged coastal area. *J. Exp. Mar. Biol. Ecol.* **228**, 209–225 (1998).
50. Pereda-Briones, L., Terrados, J., Agulles, M. & Tomas, F. Influence of biotic and abiotic factors of seagrass *Posidonia oceanica* recruitment: identifying suitable microsites. *Mar. Environ. Res.* **162**, 105076 (2020).
51. Hernán, G. et al. Future warmer seas: increased stress and susceptibility to grazing in seedlings of a marine habitat-forming species. *Glob. Change Biol.* **23**, 4530–4543 (2017).
52. Rinaldi, A. et al. The ontogeny-specific thermal sensitivity of the seagrass *Posidonia oceanica*. *Front. Mar. Sci.* **10**, 1183728 (2023).
53. Marbà, N. & Duarte, C. M. Mediterranean warming triggers seagrass (*Posidonia oceanica*) shoot mortality. *Glob. Change Biol.* **16**, 2366–2375 (2010).
54. Stipcich, P. et al. Assessment of *Posidonia oceanica* traits along a temperature gradient in the Mediterranean Sea shows impacts of marine warming and heat waves. *Front. Mar. Sci.* **9**, 895354 (2022).
55. Marín-Guirao, L., Entrambasaguas, L., Ruiz, J. M. & Procaccini, G. Heat-stress induced flowering can be a potential adaptive response to ocean warming for the iconic seagrass *Posidonia oceanica*. *Mol. Ecol.* **28**, 2486–2501 (2019).
56. Nguyen, H. M. et al. Signs of local adaptation by genetic selection and isolation promoted by extreme temperature and salinity in the Mediterranean seagrass *Posidonia oceanica*. *Mol. Ecol.* **32**, 4313–4328 (2023).
57. Telesca, L. et al. Seagrass meadows (*Posidonia oceanica*) distribution and trajectories of change. *Sci. Rep.* **5**, 1–14 (2015).
58. Boudouresque, C. F. et al. Insights into the typology of reef formations of the Mediterranean seagrass *Posidonia oceanica*. In: *Proceedings of the 5th Mediterranean Symposium on Marine Vegetation* (Portorož, Slovenia, 27-28 October 2014). Langar, H., Bouafif, C., Ouerghi, A. (edit.), RAC/SPA publ., Tunis, 58-63 (2014).
59. Spalding, M. D. et al. Marine ecoregions of the world: a bioregionalization of coastal and shelf areas. *BioScience* **57**, 573–583 (2007).
60. Garrabou, J. et al. Collaborative database to track mass mortality events in the Mediterranean Sea. *Front. Mar. Sci.* **6**, 478167 (2019).
61. Giraud, G. Recensement des floraisons de *Posidonia oceanica* (L.) Delile en Méditerranée. *Rapp. de. la Comm. Int. pour l'Exploration Scientifique de. la Mer. Méditerranée* **24**, 126–130 (1977).
62. Pergent-Martini, C. & Pergent, G. Lepidochronological analysis in the mediterranean seagrass *Posidonia oceanica* state-of-the-art and future-developments. *Oceanologica Acta* **17**, 673–681 (1994).
63. Pisano, A., Buongiorno Nardelli, B., Tronconi, C. & Santoleri, R. The new Mediterranean optimally interpolated pathfinder AVHRR SST Dataset (1982–2012. *Remote Sens. Environ.* **176**, 107–116 (2016).
64. Merchant, C. J. et al. Satellite-based time-series of sea-surface temperature since 1981 for climate applications. *Sci. Data* **6**, 1–18 (2019).
65. Bensoussan, N. et al. Using CMEMS and the Mediterranean Marine Protected Areas sentinel network to track ocean warming effects in coastal areas. *J. Operational Oceanogr.* **12**, 65–73 (2019).
66. Hobday, A. J. et al. Categorizing and naming marine heatwaves. *Oceanography* **31**, 162–173 (2018). https://www.jstor.org/stable/26542662.
67. Zhao, Z. & Marin, M. A MATLAB toolbox to detect and analyze marine heatwaves. *J. Open Source Softw.* **4**, 1124 (2019).
68. Anderson, M. J. A new method for non-parametric multivariate analysis of variance. *Austral Ecol.* **26**, 32–46 (2001).
69. Bürkner, P. C. brms: An R package for Bayesian multilevel models using Stan. *J. Stat. Softw.* **80**, 1–28 (2017).
70. Gelman, A. & Rubin, D. B. Inference from iterative simulation using multiple sequences. *Stat. Sci.* **7**, 457–472 (1992). (1992).
71. R Core Team. R: A Language and Environment for Statistical Computing. R Foundation for Statistical Computing, Vienna, Austria https://www.R-project.org/ (2023).

Acknowledgements

This work is dedicated to the memory of Monica Montefalcone, our co-author and colleague, who passed away a few days before the publication of this article. We warmly thank the management teams of Marine Protected Areas which helped in providing flowering records (Marine Natural Reserve of Cerbère-Banyuls, Nature Marine Park of the Gulf of Lions, Port-Cros National Park, Côte Bleue Marine Park, Côte Agathoise Marine Protected Area, Association Monégasque pour la Protection de la Nature), diving centres (Costa Verde Loisir, Albatros Diving, EPIR Plongée Ile Rousse, Scuba Ibiza, Blaumar Bivalvia, Federación Catalana de Actividades Subacuáticas), citizens and volunteers, in particular in the frame of the 'Observadores del mar' network https://www.seawatchers.net/ for the huge dataset made available for this work .

Author contributions

P.A.: writing, conception, data curation /analysis, figures/tables editing, data provider, review; N.B.: writing, conception, data curation /analysis, figures/tables editing, review; S.A.: writing, conception, data curation /analysis, figures/tables editing, data provider, review; C.F.B.: writing, conception, data provider, review; F.T.: writing, data provider, review; N.T.: writing, data provider, review; J.C.: data curation/analysis, figures/tables editing, review; B.B.: figures/tables editing, data provider; C.G.E.: data provider, review; B.A.: data provider, review; T.A.: data provider, review; E.A.: data provider, review; F.B.: data provider, review; J.B.: data provider, review; A.B.: data provider, review; M.C.: data provider, review; E.Ca: data provider, review; G.C.: data provider, review; T.E.: data provider, review; Y.F.T.: data provider, review; V.G.: data provider, review; S.G.: data provider, review; D.Gr. data provider, review; D.K.: data provider, review; V.M.: data provider, review; J.M.Cr: data provider, review; C.M.M.: data provider, review; H.M.: data provider, review; DM: data provider, review; J.L.S.L.: data provider, review;

T.S.: data curation/analysis, data provider; J.T.: data provider, review; G.T.J.: data provider; D.V.: data provider, review; A.Ze: data provider, review; B.A.O.: data provider; V.B.: data provider; ABD: data provider; WB: data provider; J.B.S.: data provider; JBE: data provider; C.N.B.: writing, review; IC: data provider; E.Ce: data provider; E.Cha: data provider; A.Che: data provider; E.Ch: data provider; A.Chi: data provider; G.Co: data provider; J.M.Co: data provider; I.Cv: data provider; GDA: data provider; M.D.: data provider; F.D.: data provider; M.F.C.: data provider; B.F.: data provider; R.G.: data provider; D.Gui: data provider; J.E.G.N.: data provider; A.G.: data provider; V.H: data provider; N.H.: data provider; A.I.M.: data provider; Z.J.: data provider; S.J.: data provider; O.K.: data provider; P.K.: data provider; J.K.M.: data provider; A.L.: data provider; V.L.: data provider; I.M.: data provider; G.Ma: data provider; N.M.: data provider; M.M.: data provider; N.Mi: data provider; AM: data provider; B.M.: review; C.Mo: review; P.C.N.M.: data provider; A.O.: data provider; A.Pa; data provider, review; CPM: review; A.Pe: data provider; L.P.: data provider; G.Pr: data provider, review; J.M.Re: data provider; S.Ro: data provider; J.R.: data provider; J.M.Ru: data provider; N.S.B.: data provider; M.S.F.: data provider; A.Sc: data provider; F.S.: data provider; P.S.: data provider, review; A.Zu: data provider; M.Mo: writing, data provider, review.

Funding

Fiona Tomas would like to acknowledge funding from the Government of the Balearic Islands (CAIB), under the research program "Ajudes a Projectes Biodiversitat Emmarcats dins els Plans Complementaris" through the project "Incorporación de nuevas tecnologías en la caracterización del estado de conservación de los bosques submarinos de Baleares y su contribución a servicios ecosistémicos (BIO022 PRTR BIODIV ConBoSerBio)". IMEDEA is an accredited "Maria de Maeztu Excellence Unit" (Grant CEX2021-001198, funded byMICIU/AEI/10.13039/501100011033). Núria Teixidó was supported by the French government through the National Research Agency Investments for the Future ("4Oceans-Make Our Planet Great Again" grant, ANR-17-MOPGA-0001) and the European Union NextGeneration EU (PIANO NAZIONALE DI RIPRESA E RESILIENZA (PNRR) – MISSIONE 4 COMPONENTE 2, "Dalla ricerca all'impresa" INVESTIMENTO 1.4 – D.D. 1034 17/06/2022, CN00000033). Jérémy Carlot was supported by a Beatriu de Pinós postdoctoral fellowship (2024 BP 00106), funded by the Government of Catalonia and co-funded by the European Union under the Marie Skłodowska-Curie COFUND programme. Jordi Boada acknowledges funding received by the H2020 program (MSCA-IF SHIFT2SOLVEXXX), and by the I + D + i project RYC2021-033650-I and PID2022-140652NA-I00 MITnPOINT funded by the MCIN/AIEI/10.13039/501100011033 and FEDER. Jorge Terrados would like to acknowledge the research contracts "Restoration of *Posidonia oceanica* meadow, REE Marine Forest" funded by Redeia (Spain) and "High-quality sequencing of *Posidonia oceanica* genome" funded by Iberostar Foundation (Spain). Andres Izquierdo study forms part of the ThinkInAzul programme and was supported by MCIN with funding from European Union NextGenerationEU (PRTR-C17.I1) and by Generalitat Valenciana (GVA-THINKINAZUL/2021/016; F. Gimenez-Casalduero, UA). Daniele Grech was supported by the LIFE PINNA (LIFE20 NAT/IT/001122) "Conservation and re-stocking of the *Pinna nobilis* in the western Mediterranean and Adriatic Sea" and Sea Urchin monitoring program (*Paracentrotus lividus*) funded by the Autonomous Region of Sardinia (RAS). He would like also to thank the entire citizen science underwater group "Subacquei per la Scienza" for flowering sightings. In Andalusia (Spain), the authors are grateful to Eugenio Montes and Soledad Vivas, responsible in the Junta de Andalucía for the Sustainable Marine Environment Management Program, and to the rest of the team members, as well as to Alejandra Pérez and Fernando Orri from Aquatours for coordinating the work of the volunteers at the Aguadulce and Cerrillos stations (Almería). Arturo Zenone was funded under the National Recovery and Resilience Plan (NRRP), Mission 4 Component 2 Investment 1.4 - Call for tender No. 3138 of 16 December 2021, rectified by Decree n.3175 of 18 December 2021 of Italian Ministry of University and Research funded by the European Union – NextGenerationEU. Project code CN_00000033, Concession Decree No. 1034 of 17 June 2022 adopted by the Italian Ministry of University and Research, CUP B83C22002930006 (CNR). Arnaud Boulenger was supported by the University of Liege (Belgium) and the Fonds National de la Recherche Scientifique - FNRS (grants ASP 40006932 and CDR J.0076.23). Periklis Kleitou, George Constantinou and Demetris Kletou (MER) are grateful to Christina Michail (MER) and Melina Marcou (DFMR) for documenting and providing information about flowering events in Cyprus. Eugenia T. Apostolaki and Catalina A. Garcia-Escudero acknowledge supported by DRESSAGE (No MIS5045792 through the Operational Program 'Competitiveness, Entrepreneurship and Innovation' (EPAnEK 2014-2020, NSRF), CHRISI ('Implementation of measures for the Action Plan of Chrisi island, Cretan Sea' funded by Region of Crete) and AGOGOS (No 81/10.4.23 HCMR own funding) projects. Vesna Mačić would like to thank to RAC SPA for support in implementation of national monitoring program in line with the IMAP, MoU N°22/2024-SPA/RAC We are deeply thankful to T-Med Network for providing temperature analyses at the Mediterranean scale.

Competing interests

The authors declare no competing interests.

Additional information

Supplementary information The online version contains supplementary material available at https://doi.org/10.1038/s43247-026-03631-8.

Correspondence and requests for materials should be addressed to Patrick Astruch.

Peer review information *Communications Earth & Environment* thanks Jennifer L. Ruesink and the other, anonymous, reviewer(s) for their contribution to the peer review of this work. Primary Handling Editors: Vasco Vieira and Alice Drinkwater. A peer review file is available

Patrick Astruch[1] ✉, Nathaniel Bensoussan[2], Serena André[1], Charles-François Boudouresque[3], Fiona Tomas[4], Núria Teixidó[5,6], Jérémy Carlot[7], Bruno Belloni[1], Catalina A. Garcia-Escudero[8], Barış Akçalı[9], Teresa Alcoverro[10], Eugenia T. Apostolaki[8], Fabio Badalamenti[11,12], Jordi Boada[10], Arnaud Boulenger[13,14], Mélanie Cabral[1], Edoardo Casoli[15], Giovanni Chimienti[16], Tristan Estaque[17], Yolanda Fernández Torquemada[18], Vasilis Gerakaris[19], Sylvie Gobert[13,14], Daniele Grech[20], Demetris Kletou[21], Vesna Mačić[22], Julia Máñez-Crespo[4], Candela Marco-Méndez[10], Heike Molenaar[23], Diego Moreno[24], José Luis Sánchez-Lizaso[18], Thomas Schohn[1], Jorge Terrados[4], Georgina Torras Jorda[25], Daniele Ventura[15], Arturo Zenone[5,11,12], Balma Albalat-Oliver[26], Vincent Bardinal[27], Agustín Barrajón Domenech[24], Walid Belgacem[28], Jamila Ben Souissi[29], Jaime Bernardeau-Esteller[30], Carlo Nike Bianchi[31], Inés Castejón[4], Emma Cebrian[10], Eric Charbonnel[32], Adrien Cheminée[17], Edouard Chéré[33], Antonia Chiarore[5], George Constantinou[21], Jean-Michel Cottalorda[23], Ivan Cvitković[34], Giovanni D'Anna[12,35], Marija Despalatović[34], Fedra Dokoza[36], Manuel Fernández-Casado[24], Bruno Ferrari[37], Raouia Ghanem[29], Dorian Guillemain[3], Juan Eduardo Guillén Nieto[38], Aysu Güresen[39], Virginie Hartmann[40], Noelia Hernandez[41], Muñoz Andres Izquierdo[18,42], Zrinka Jakl[36], Stéphane Jamme[43], Onur Karayalı[44], Periklis Kleitou[21], Jelena Kurtović Mrčelić[45], Arthur Lazennec[1], Valentina Lovat[46], Ilaria Mancini[47], Gianluca Mancini[15], Núria Marbà[4], Michel Marengo[14], Noëmie Michez[37], Alice Mirasole[5], Briac Monnier[48,49], Carla Morri[31], Pedro C. Navarro-Martinez[30], Alice Oprandi[47], Arianna Pansini[50], Christine Pergent-Martini[1,48], Alexis Pey[51], Luigi Piazzi[52], Gabriele Procaccini[5], José Miguel Remón[24], Stéphane Roberty[53], Javier Romero[54], Juan Manuel Ruiz[30], Neus Sanmarti Boixeda[54], Manu Sant Felix[40], Antonio Scannavino[55], Francisco Sobrado[25], Patrizia Stipcich[12,50,56], Ante Žuljević[34] & Monica Montefalcone[12,47]

[1]GIS Posidonie, Aix-Marseille University, OSU Pythéas, Campus of Luminy, Marseille, France. [2]University of Brest, CNRS, Ifremer, IRD, Laboratoire d'Océanographie Physique et Spatiale (LOPS), IUEM, Plouzané, France. [3]Aix-Marseille University and University of Toulon, MIO (Mediterranean Institute of Oceanography), IRD, CNRS, Campus of Luminy, Marseille, France. [4]Mediterranean Institute of Advanced Studies IMEDEA (CSIC-UIB), Mallorca, Spain. [5]Stazione Zoologica Anton Dohrn, National Institute of Marine Biology, Ecology and Biotechnology, Ischia Marine Center, Naples, Italy. [6]Laboratoire d'Océanographie de Villefranche, Sorbonne Université, CNRS, Villefranche-sur-Mer, France. [7]Centro Oceanográfico de Baleares, IEO, CSIC, Palma de Mallorca, Spain. [8]Institute of Oceanography, Hellenic Centre for Marine Research, Heraklion, Crete, Greece. [9]University of Dokuz Eylul Institute of Marine Sciences & Technology Haydar Aliyev, Izmir, Turkey. [10]Centre d'Estudis Avançats de Blanes- CEAB, CSIC, Blanes, Spain. [11]Institute for the Study of Anthropogenic Impacts and Sustainability in Marine Environment, National Research Council, (IAS-CNR), Palermo, Italy. [12]NBFC, National Biodiversity Future Centre, Palermo, Italy. [13]Université de Liège, Centre MARE, Focus, Laboratoire d'Océanologie, Liège, Belgium. [14]STAtion de Recherche Sous-marines et Océanographiques (STARESO), Calvi, France. [15]Department of Environmental Biology, Sapienza University of Rome, Rome, Italy. [16]Department of Biosciences, Biotechnologies and Environment, University of Bari Aldo Moro, Bari, Italy. [17]Septentrion Environnement, Campus Nature Provence, Lycée Professionnel Agricole des Calanques, Marseille, France. [18]Department of Marine Sciences and Applied Biology, University of Alicante, Alicante, Spain. [19]Institute of Oceanography, Hellenic Centre for Marine Research (HCMR), Athens, Greece. [20]IMC - International Marine Centre, Oristano, Italy. [21]Marine & Environmental Research (MER) Lab, Limassol, Cyprus. [22]Institute of marine biology, University of Montenegro, Kotor, Montenegro. [23]Université Côte d'Azur, CNRS, ECOSEAS UMR7035, Nice, France. [24]Agencia de Medio Ambiente y Agua de Andalucía/ Consejería de Sostenibilidad y Medio Ambiente/ Junta de Andalucía, Sevilla, Spain. [25]Albatros diving, Cala bona, Spain. [26]Grup d'Estudis de la Naturalesa – Grup Ornitològic Balear (GEN-GOB), Eivissa, Spain. [27]Parc national de Port-Cros, Hyères, France. [28]Association Méditerranée Action Nature/ Unité de cogestion de l'AMCP de la Galite (MAN-APAL-The Med Fund), Bizerte, Tunisia. [29]National Institute of Agronomy of Tunisia (INAT), University of Tunis El Manar, Biodiversity, Biotechnologies and Climate Change Laboratory (LR11ES09), Tunis, Tunisia. [30]Centro Oceanográfico de Murcia, Instituto Español de Oceanografía, Murcia, Spain. [31]Department of Integrative Marine Ecology (EMI), Stazione Zoologica Anton Dohrn - National Institute of Marine Biology, Ecology and Biotechnology, Genoa Marine Centre (GMC), Genova, Italy. [32]Parc Marin de la Côte Bleue, Observatoire Plage du Rouet, Carry-le-Rouet, France. [33]Ville d'Agde, Direction Gestion du milieu marin, Aire Marine Protégée de la côte agathoise, Agde, France. [34]Institute of Oceanography and Fisheries (IZOR), Split, Croatia. [35]Istituto per lo studio degli impatti Antropici e sostenibilità in ambiente Marino, Consiglio Nazionale delle Ricerche (IAS-CNR), Castellammare del Golfo, Italy. [36]Sunce, Split, Croatia. [37]Parc naturel marin du golfe du Lion / Office français de la biodiversité, Argelès-sur-Mer, France. [38]Instituto de Ecologia Litoral, Alicante, Spain. [39]University of Istanbul, Faculty of Aquatic Sciences, Istanbul, Turkey. [40]Réserve Naturelle Marine de Cerbère-Banyuls, Banyuls sur mer, France. [41]Vellmarí Association, Formentera, Balearic Islands, Spain. [42]Marine Research Center of Santa Pola (CIMAR), University of Alicante, Alicante, Spain. [43]Aquanaute expertise, Antibes, France. [44]Ege University Faculty of Fisheries, Erzene Mah. Bornova İzmir, İzmir, Türkiye. [45]Public Institution Sea and Karst, Split, Croatia. [46]UNESCO Regional Bureau for Science and Culture in Europe, Venice, Italy. [47]Seascape Ecology Laboratory, DiSTAV (Department of Earth, Environment and Life Sciences), University of Genoa, Genova, Italy. [48]Université de Corse Pasquale Paoli, UMR CNRS SPE 6134, Faculté des Sciences et Techniques Campus Grimaldi, Corte, France. [49]Université de Corse Pasquale Paoli, UAR CNRS 3514 Plateforme Marine Stella Mare, Biguglia, Corse, France. [50]Department of Chemical, Physical, Mathematical and Natural Sciences, University of Sassari, Sassari, Italy. [51]Thalassa Marine Research & Environmental Awareness, Tourrette-Levens, France. [52]Centro Interuniversitario di Biologia Marina ed Ecologia Applicata 'G. Bacci', Livorno, Italy. [53]InBioS - Animal Physiology and Ecophysiology, Department of Biology, Ecology and Evolution, University of Liège, Liège, Belgium. [54]Departament de Biologia Evolutiva, Ecologia i Ciències Ambientals Secció d'Ecologia, Barcelona, Spain. [55]Dipartimento di scienze della terra e del mare (DISTEM), Università degli studi di Palermo, Palermo, Italy. [56]Department of Biology, University of Naples Federico II, Naples, Italy.

✉e-mail: patrick.astruch@univ-amu.fr